Check for updates

View Article Online
View Journal

Nanoscale

Accepted Manuscript

This article can be cited before page numbers have been issued, to do this please use: S. Zhang, K. E.S. Nassar, A. Azmy, L. Wojtas, I. Spanopoulos and Q. Tu, *Nanoscale*, 2026, DOI: 10.1039/D6NR00361C.

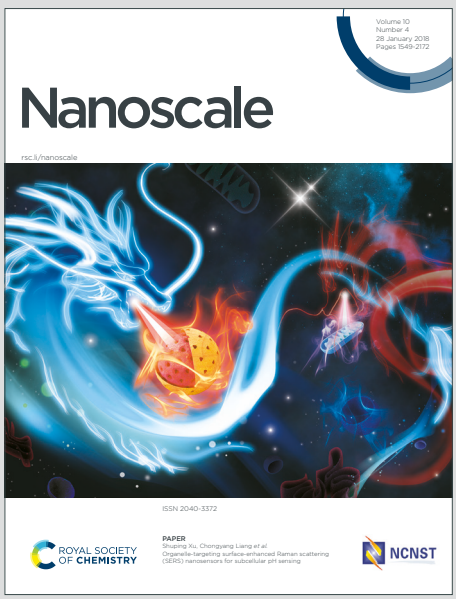

This is an Accepted Manuscript, which has been through the Royal Society of Chemistry peer review process and has been accepted for publication.

Accepted Manuscripts are published online shortly after acceptance, before technical editing, formatting and proof reading. Using this free service, authors can make their results available to the community, in citable form, before we publish the edited article. We will replace this Accepted Manuscript with the edited and formatted Advance Article as soon as it is available.

You can find more information about Accepted Manuscripts in the Information for Authors.

Please note that technical editing may introduce minor changes to the text and/or graphics, which may alter content. The journal's standard Terms & Conditions and the Ethical guidelines still apply. In no event shall the Royal Society of Chemistry be held responsible for any errors or omissions in this Accepted Manuscript or any consequences arising from the use of any information it contains.

ROYAL SOCIETY OF CHEMISTRY

rsc.li/nanoscale

View Article Online
DOI: 10.1039/D6NR00361C

In-Plane Mechanical Property of Terephthalate-based Two-Dimensional Metal-Organic Frameworks

Shengjia Zhang,[a#] Kamal E. S. Nassar,[b#] Ali Azmy,[b] Lukasz Wojtas,[b] Ioannis Spanopoulos,[b] and Qing Tu[a*]*

[a] *Department of Material Science and Engineering, Texas A&M University*

[b] *Department of Chemistry, University of South Florida, Tampa, FL, 33620*

 # these authors contributed equally

** corresponding authors: spanopoulos@usf.edu; qing.tu@tamu.edu.*

Keywords: 2D-MOF, AFM stretching, in-plane, elastic modulus, structure-property relationship

Open Access Article. Published on 13 April 2026. Downloaded on 4/14/2026 3:06:08 PM.
This article is licensed under a Creative Commons Attribution-NonCommercial 3.0 Unported Licence.

Nanoscale Accepted Manuscript

Abstract

Two-dimensional (2D) metal-organic frameworks (MOFs) are often subjected to mechanical loading in their applications, and the in-plane elastic modulus $E_{\parallel}$ is a critical material property needed to understand and predict the mechanical behaviors of 2D MOFs for improved mechanical reliability and strain engineering of their functional properties. However, the $E_{\parallel}$ of 2D MOFs are largely unknown, even for those with widely used coordination linkers like 1,4-benzenedicarboxylate (BDC), because of the challenges in in-plane mechanical testing imposed by both the extreme dimensionality and the high sensitivity of 2D MOFs to external factors (*e.g.*, e-beams) due to their hybrid organic-inorganic nature. Here we employ atomic force microscopy (AFM) stretching suspended thin membranes to measure $E_{\parallel}$ of three structurally related, BDC-coordinated MOFs. The 2D $Zn_3(BDC)_3(H_2O)_2 \cdot 4(DMF)$

View Article Online
DOI: 10.1039/D6NR00361C

(DMF = N,N-Dimethylformamide) has an $E_{\parallel}$ of 11.2 ± 2.5 GPa, much lower than that of its 3D analog, $(DMA)_2[Zn_3(BDC)_4 \cdot 1.5H_2O]$ (DMA = dimethylammonium) ($E_{\parallel}$ = 25.9 ± 6.3 GPa), owing to the absence of interlayer covalent bonding. However, a 2D Mn analog, $Mn_3(BDC)_3 \cdot 4(DMF)$, exhibits enhanced in-plane stiffness ($E_{\parallel}$ = 25.5 ± 4.9 GPa), likely originating from the strengthened coordination at the nodes. We further compare 2D MOFs to other 2D materials and widely-used engineering material systems using a density *vs.* $E_{\parallel}$ Ashby plot. Our results provide indispensable insights into the structure-mechanical-property relationship of 2D MOFs to guide material engineering/selection.

Open Access Article. Published on 13 April 2026. Downloaded on 4/14/2026 3:06:08 PM.
This article is licensed under a Creative Commons Attribution-NonCommercial 3.0 Unported Licence.

Nanoscale Accepted Manuscript

View Article Online
DOI: 10.1039/D6NR00361C

Open Access Article. Published on 13 April 2026. Downloaded on 4/14/2026 3:06:08 PM.
This article is licensed under a Creative Commons Attribution-NonCommercial 3.0 Unported Licence.

Nanoscale Accepted Manuscript

Introduction

Metal-organic frameworks (MOFs) are a family of porous crystalline materials that combine metal ions with coordinated organic ligands to form complex structures enabling huge potential in a wide range of applications, including gas storage, catalysis, and chemical separations.[1-4] The tremendous chemical space available to these materials, together with the solution processability, allows for facile design of MOF structures with tailored functionality.[5] The success of two-dimensional (2D) materials further inspired the engineering of MOFs into 2D layered compounds to relax the structural constraints and expand the functional property and architectural design space.[6-8] Integration of MOFs and other low-dimensional materials into novel heterostructures *via* clean van der Waals (vdW) interfaces is thus possible and has resulted in new promising applications.[6, 9] Hence, interlayer interfaces become a new playground for tuning material properties (*e.g.*, intercalation, sliding).[6]

In all these applications, 2D MOFs are often subjected to mechanical loading during device fabrication and operations,[10-12] such as compression, dilation, stretching, bending, twisting, *etc*., where elastic modulus E is a critical mechanical property needed to understand and predict the mechanical behaviors of 2D MOFs in order to mitigate mechanical failure and improve the mechanical reliability of MOF-based applications. Moreover, mechanical strain can also be harnessed to enhance the functional performance of 2D MOFs or to tailor the properties of the materials interfacing with 2D MOFs.[6, 13, 14] Knowing E of 2D MOFs is the first step to achieve precisely controlled strain engineering. The abundant chemistry involving

View Article Online
DOI: 10.1039/D6NR00361C

hybrid organic-inorganic bonds, which differ from those in conventional materials such as metals, ceramics, and polymers,[10, 15] further calls for the exploration of the structure-property relationships of 2D MOFs regarding their mechanical behavior.

Because of both the fundamental importance and practical need, significant efforts have been devoted to studying the mechanical properties of 3D MOFs,[10, 11] mainly utilizing small-scale mechanical techniques like instrumented nanoindentation and atomic force microscopy (AFM) due to the small sample size, though the mechanical study still significantly lags behind other functional property studies of these materials. Such small-scale techniques are applicable to study the out-of-plane (*i.e.*, perpendicular to the basal planes of the molecular sheets) mechanical properties of 2D MOFs, owing to the layered structure. However, evaluating the in-plane mechanical properties is more challenging. First, directly applying nanoindentation or AFM-based indentation techniques along the in-plane directions violates the assumptions of analysis methods due to the in-plane *vs.* out-of-plane mechanical anisotropy of these materials.[16, 17] Although many studies still employed these indentation techniques neglecting this fact to probe the in-plane directions,[12, 18-20] the reported results are questionable. Second, the small sample size and high susceptibility to damage from other factors in the test (*e.g.*, electron beams or humidity) render many in-plane testing techniques widely used in 2D materials not feasible for 2D MOFs. Because of these challenges, only a handful of reliable reports about the in-plane mechanical property of 2D MOFs are available in the literature to date,[21-26] despite that in-plane is the main loading directions for 2D MOFs in practical

Open Access Article. Published on 13 April 2026. Downloaded on 4/14/2026 3:06:08 PM.
This article is licensed under a Creative Commons Attribution-NonCommercial 3.0 Unported Licence.

Nanoscale Accepted Manuscript

View Article Online
DOI: 10.1039/D6NR00361C

Open Access Article. Published on 13 April 2026. Downloaded on 4/14/2026 3:06:08 PM.
This article is licensed under a Creative Commons Attribution-NonCommercial 3.0 Unported Licence.

applications owing to the layered structure. While 2D MOFs and the corresponding 3D counterparts can share the same metal-organic bonds and connection architecture in-plane,[6] where the metal-organic-ligand architecture, rather than the weak van der Waals (vdW) interface (as in the out-of-plane direction), is still the main load carrier, it remains unclear how the transition of the structure from 3D to 2D will affect the in-plane elastic modulus $E_{\parallel}$. This is largely due to the lack of direct comparison of the in-plane elastic moduli of 2D and 3D MOFs. This knowledge gap hinders our ability to leverage the abundant structure-mechanical-property study of the 3D MOFs[10-12] for designing 2D analogs. Furthermore, although it is common to substitute the metal ions in the MOF structure while maintaining the coordination ligands and topology,[6] the influence of such modification on $E_{\parallel}$ of 2D MOFs is still elusive.

Here, we measure $E_{\parallel}$ of 2D MOF coordinated by the 1,4-benzenedicarboxylate (BDC) linker. This is one of the most widely used organic linkers in MOF chemistry.[27] Its rigid and linear geometry supports predictable coordination environments and reproducible framework topologies,[28] which have enabled the development of numerous benchmark MOF systems such as MOF-5[29] and UiO-66.[30] Therefore, BDC-based frameworks provide a structurally reliable and broadly representative platform for probing the intrinsic mechanical behavior of layered MOFs and establishing insights that are transferable to other 2D coordination polymer systems.[28] However, to date, the mechanical properties of 2D MOFs based on BDC linker have not been investigated.[11]

We use AFM stretching suspended thin 2D MOF membranes to measure their

Nanoscale Accepted Manuscript

View Article Online
DOI: 10.1039/D6NR00361C

$E_{\parallel}$. This method has been used to reliably quantify $E_{\parallel}$ of various 2D materials,[31-34] including 2D materials with hybrid bonds[35, 36] or coordinated polymers[37] similar to 2D MOFs. We first compare $E_{\parallel}$ of 2D MOF $Zn_3(BDC)_3(H_2O)_2 \cdot 4(DMF)$ (DMF = N,N-Dimethylformamide) to its 3D analog, $(DMA)_2[Zn_3(BDC)_4 \cdot 1.5H_2O]$ (DMA = dimethylammonium), to uncover the impact of structural transition from 3D to 2D on the elastic property. Furthermore, we replace Zn with Mn in the 2D MOF while maintaining the same framework connectivity to examine the effects of metal ions on the elastic modulus. These measurements, together with the comparison with other relevant layered materials and classical materials widely adopted in engineering applications, provide indispensable insights into the in-plane structure-mechanical-property relationship of 2D MOFs and materials selection for applications.

Experimental Section

Materials Synthesis. All MOF materials were synthesized by solution-based methods and characterized by single crystal and powder X-ray diffraction (XRD) to confirm the success of synthesis (**Figs. 1** and **2**, and **Supporting Information (SI) – Section 1**). All the chemicals were purchased from Sigma-Aldrich and used as received without any further purification. Briefly, for 3D MOF, $(DMA)_2[Zn_3(BDC)_4 \cdot 1.5H_2O]$ (abbreviated as 3D-Zn-MOF below), 0.07 mmol terephthalic acid were dissolved in 3 mL DMF and 1 mL ethanol in a 20 ml glass vial under heating (150 °C hot plate temperature indication). Then, 0.07 mmol of

Open Access Article. Published on 13 April 2026. Downloaded on 4/14/2026 3:06:08 PM.
This article is licensed under a Creative Commons Attribution-NonCommercial 3.0 Unported Licence.

Nanoscale Accepted Manuscript

View Article Online
DOI: 10.1039/D6NR00361C

Open Access Article. Published on 13 April 2026. Downloaded on 4/14/2026 3:06:08 PM.
This article is licensed under a Creative Commons Attribution-NonCommercial 3.0 Unported Licence.

$Zn(NO_3)_2 \cdot 6H_2O$ and three drops of concentrated nitric acid were added. The heating decomposed DMF into DMA, which served as counter cations to stabilize and charge balance the structure. The solution was then kept at 85 °C overnight in an isothermal oven, yielding colorless crystals upon cooling to room temperature. This growth method was then slightly modified to produce 2D MOF, $Zn_3(BDC)_3(H_2O)_2 \cdot 4(DMF)$ (abbreviated as 2D-Zn-MOF below). In this case, 0.07 mmol terephthalic acid were dissolved in 6 mL DMF and 1 mL ethanol under sonication. After adding one drop of nitric acid and 0.07 mmol $Zn(NO_3)_2 \cdot 6H_2O$, the mixture was heated at 85 °C in an isothermal oven overnight to yield transparent crystals. The synthesis of 2D $Mn_3(BDC)_3 \cdot 4(DMF)$ (abbreviated as 2D-Mn-MOF below) followed a published protocol.[38]

AFM Stretching Suspended MOF Membranes. The AFM experiments were conducted following our reported protocol.[35, 39] Briefly, thin MOF membranes were mechanically exfoliated via scotch tape[40] and transferred to freshly cleaned SiO_2/Si wafer with patterned holes inside a N_2-filled glovebox. The exfoliation is very straightforward for 2D MOFs owing to the weak interlayer interfaces in the crystals (**Figs. 1C**). We found that the 3D-Zn-MOF can also be exfoliated by this method, producing thin membranes with crystal orientations similar to 2D-Zn-MOF, probably because the interlayer bonds are not that strong and the density of the bonds are not high (see **Fig. 1F**). However, such interlayer bonds are still much stronger than the vdW interactions in 2D-Zn-MOF, which results in a much lower yielding rate of successful transfer of 3D-Zn-MOF than the 2D version.

Nanoscale Accepted Manuscript

View Article Online
DOI: 10.1039/D6NR00361C

Open Access Article. Published on 13 April 2026. Downloaded on 4/14/2026 3:06:08 PM.
This article is licensed under a Creative Commons Attribution-NonCommercial 3.0 Unported Licence.

All AFM measurements are performed using an Asylum MFP-3D Infinity AFM (Asylum Research, Oxford Instruments, CA) with AC240TS (Olympus) probes under dry air flow. Before the AFM measurements, the deflection sensitivity of the AFM cantilever is calibrated by recording the indentation force curve of the cantilever on clean silicon surface. The spring constant k_c of the AFM cantilever is then calibrated by fitting the first free resonance peak of the cantilever to the simple harmonic oscillator equation[41] to measure the power spectral density of the thermal noise fluctuations in air.[42] The indentation rate was kept at 100 nm/s to avoid high-rate-induced noise.[35] The membranes with hysteresis or sliding features in the loading and unloading curves are excluded. At least 10 membranes from two distinct crystals were measured for each type of MOF tested here.

Results and Discussion

Targeting the synthesis of 2D MOFs, we selected Zn-based analogs on BDC ligands, which are extensively explored. The 2D-Zn-MOF and the 2D-Mn-MOF have been reported in literature before,[38, 43] as well as the framework of the 3D-Zn-MOF.[44] However, the reported structure of the latter, does not have the correct formula necessary for a charge balanced structure. Hence, in this work, we synthesized and characterized the material by XRD to identify the correct structure and formula, given their importance for understanding underlying structure-property relationships, especially given the ultra-fine nature of the targeted mechanical properties. We note that, in this work, we use the 2D and 3D notation to refer to the degree of

Nanoscale Accepted Manuscript

View Article Online
DOI: 10.1039/D6NR00361C

Open Access Article. Published on 13 April 2026. Downloaded on 4/14/2026 3:06:08 PM.
This article is licensed under a Creative Commons Attribution-NonCommercial 3.0 Unported Licence.

coordination of the MOF.[45] In a 2D MOF, coordination bonds will span across two directions forming layers, which would not be connected through coordination bonds, rather through weak interactions. In a 3D MOF, coordination bonds extend in all three spatial directions. Therefore, the use of the terms 2D and 3D MOF does not refer to exfoliated single-layer frameworks. The flakes used in the mechanical studies contain multiple layers of the corresponding 2D and 3D MOFs (see below in the mechanical test part), not a single constituent layer of the materials.

By adjusting the reaction conditions, we managed to synthesize a 2D and a 3D Zn-based frameworks. Starting with the structure of the 2D-Zn-MOF, it was determined by single-crystal X-ray diffraction (SC-XRD) studies that the material crystalized in the centrosymmetric space group $P2_1/c$ with the formula $C_{36}H_{44}N_4O_{18}Zn_3$. The secondary building unit of the structure features a trinuclear metallic cluster consisting of three Zn^{2+} cations, four terephthalic acid (BDC) molecules and two water molecules. The Zn^{2+} cations are vertically aligned across the layer and connected through the carboxylate groups of BDC. The central Zn^{2+} cation is in centrosymmetric octahedral coordination with six oxygen atoms derived from six different carboxylate groups, whereas the two terminal Zn^{2+} cations have a coordination number of 4 instead of 6 where three oxygen atoms derived from three carboxylate groups are coordinated to the Zn^{2+} cation and the metal node is terminated with one water molecule (**Fig. 1A**). The structure is completed with two DMF solvent molecules that hydrogen bonded to each of the terminal water molecules of the metal nodes at a distance of 1.75Å, giving rise to the layered 2D framework

Nanoscale Accepted Manuscript

View Article Online
DOI: 10.1039/D6NR00361C

with an overall formula of $Zn_3(BDC)_3(H_2O)_2 \cdot 4(DMF)$ shown in (**Figs. 1B, C**). By examining the bonding scheme of the metal clusters, it was found that Zn-O bond length ranges from 2.035 Å to 2.204 Å for the central octahedron, whereas Zn-O bond lengths in the terminal tetrahedra were found to be 1.940 Å, 1.944 Å, 1.967 Å, and 2.009 Å. While the distance between adjacent Zn^{2+} cations within the same trinuclear metal cluster is 3.249 Å, Zn metal clusters lie at a distance of 10.41 Å measured between the central Zn cations of the clusters. Moreover, the 2D layers are stacked across the *bc-plane*, with a closest distance of 4.62 Å between the terminating water molecules of the metal cluster, while DMF molecules lie between the layers and connect them through hydrogen bonding.

Shifting the focus to the 3D structure, it was shown from SC-XRD that the material crystallized in the c-centered monoclinic *C*2/*c* space group having a twofold rotation axis perpendicular to two glide planes with the formula $C_{36}H_{32}N_2O_{17.5}Zn_3$. The structure features the same metal cluster as the 2D material discussed above with the exception of replacing the two terminal water molecules with one monodentate terephthalic acid (BDC) molecule bridging between the layers forming a 3D framework (**Figs. 1E**, **1F**). Consequently, the metal cluster of this structure consists of three Zn^{2+} cations with two different coordination modes similar to the 2D structure in which the central cation is coordinated to six oxygen atoms of six different BDC molecules that are shared with other Zn^{2+} cations forming an octahedron, whereas the two terminal metal cations are coordinated to four oxygens derived from four BDC molecules forming tetrahedra and connecting the metal nodes across the three

Open Access Article. Published on 13 April 2026. Downloaded on 4/14/2026 3:06:08 PM.
This article is licensed under a Creative Commons Attribution-NonCommercial 3.0 Unported Licence.

Nanoscale Accepted Manuscript

View Article Online
DOI: 10.1039/D6NR00361C

dimensions with two disordered protonated DMA molecules inside the cavity forming a 3D framework with overall formula $(DMA)_2[Zn_3(BDC)_4 \cdot 1.5H_2O]$ (**Fig. 1D**). In terms of bonding scheme, Zn-O bond lengths for the central and terminal clusters are almost identical to those of the 2D structure. Specifically, Zn-O bond length of the central octahedron ranges from 2.037 Å to 2.244 Å while the bond lengths of the two terminal tetrahedra are 1.947 Å, 1.965 Å, 1.976 Å, and 1.985 Å. Furthermore, the interatomic distances between the metal centers are also similar to those of the 2D structure, where the distance between the central and terminal Zn^{2+} cations is 3.266 Å, and the distance between the closest terminal metal cations of two different metal clusters is 10.36 Å.

Notably, the 2D-Zn-MOF and 2D-Mn-MOF share an almost identical structure[38] (**Figs. 1C** and **S1B**), except that 2D-Zn-MOF contains some H_2O molecules in the cavities while 2D-Mn-MOF does not (see the chemical formula in the synthesis part). Powder XRD (PXRD) measurements were used to confirm phase purity (**Fig. 2**), revealing that the calculated and experimental PXRD patterns are identical.

Fig. 3 illustrates the distinct coordination environments of the three employed MOF herein: 2D-Zn-MOF, 3D-Zn-MOF, and 2D-Mn-MOF. The two Zn-based MOFs share structural similarities but differ primarily in their terminal ligands. In 2D-Zn-MOF, aqua ligands (H_2O) serve as terminal linkers, while the Zn^{2+} centers in 3D-Zn-MOF coordinate exclusively with BDC linkers, which bridge adjacent layers covalently (**Figs. 3A and B**). Consequently, the layers of 2D-Zn-MOF, though terminated by aqua ligands, are held together by vdW interactions, yielding a

Open Access Article. Published on 13 April 2026. Downloaded on 4/14/2026 3:06:08 PM.
This article is licensed under a Creative Commons Attribution-NonCommercial 3.0 Unported Licence.

Nanoscale Accepted Manuscript

View Article Online
DOI: 10.1039/D6NR00361C

Open Access Article. Published on 13 April 2026. Downloaded on 4/14/2026 3:06:08 PM.
This article is licensed under a Creative Commons Attribution-NonCommercial 3.0 Unported Licence.

Nanoscale Accepted Manuscript

two-dimensional architecture with weak interlayer interactions. In contrast, the layers of 3D-Zn-MOF are covalently interconnected through BDC linkers, giving rise to a fully three-dimensional framework (**Fig. 3B**). The 2D-Mn-MOF presents a markedly different structural motif at the coordination nodes. It is built around a trinuclear metal cluster in which all three Mn^{2+} centers are six-coordinate, yet with differentiated ligand environments. The central Mn^{2+} octahedron is coordinated exclusively by six BDC linkers, whereas each of the two terminal Mn^{2+} octahedra coordinates with three BDC linkers and two DMF molecules, with the latter acting as terminal ligands that enforce layer separation and stabilization through vdW interactions (**Fig. 3C**).

Thin flakes of MOF transferred to the patterned silicon wafer was first identified by an optical microscope (*e.g.*, **Figs. 4B, S2A** and **S2E**). The flakes were then imaged by tapping mode AFM (**Figs. 4C, S2B** and **S2F**) to measure the thickness of the membrane and precisely position the AFM tip to the center of the membrane for nanomechanical test as illustrated in **Fig. 4A**. Membranes with a thickness between 10 to 30 nm (**Figs. 4C** (**inset**), **S2D** and **S2H**) were selected for test because (1) the flake is sufficiently thick to ensure any softening effects due to potential interlayer sliding will be saturated and the measured $E_{\parallel}$ represents the values of the bulk crystals,[32, 35, 46] as further confirmed by no clear thickness dependence of $E_{\parallel}$ in the tested range (**Fig. S3**); and (2) the flake is thin enough such that the widely used analysis model is still applicable.[31, 35, 47] As the AFM tip stretched the center of the membrane in Z direction, the applied force F and the total moving distance of the piezo in the vertical direction Z_{piezo} were collected. The membrane's actual deformation δ is

View Article Online
DOI: 10.1039/D6NR00361C

Open Access Article. Published on 13 April 2026. Downloaded on 4/14/2026 3:06:08 PM.
This article is licensed under a Creative Commons Attribution-NonCommercial 3.0 Unported Licence.

Nanoscale Accepted Manuscript

then determined as:

$$\delta = Z_{Piezo} - \delta_{tip} \quad (1)$$

where $\delta_{tip} = F/k_c$ represents the deflection of the AFM tip.

Under such loading condition, the deformation of the suspended MOF membrane can be modeled as an isotropic continuous circular membrane with fixed edges and a point load in the center,[34, 48] whose $F-\delta$ curve is described by Equation (2) below:[34, 39, 46]

$$F - F_0 = \left[\frac{4\pi E_{\parallel} t^3}{3(1-\nu^2)a^2}\right](\delta - \delta_0) + \sigma_0^{2D}\,\pi(\delta - \delta_0) + \frac{q^3 E_{\parallel} t}{a^2}(\delta - \delta_0)^3, \quad (2)$$

where t and a are the thickness and radius of the membrane, respectively; σ_0^{2D} represents the pre-tension in the membrane due to transfer; F_0 and δ_0 indicate the actual contact point when the AFM tip starts to stretch the membrane; and $q = 1/(1.05 - 0.15\nu - 0.16\nu^2)$ with ν being the Poisson's ratio of the material. Here, we take ν = 0.3, which is commonly accepted for hybrid organic-inorganic framework materials like MOFs and hybrid organic-inorganic perovskites (HOIPs).[10, 35, 49] The first term represents the bending of the membrane while the 2nd term is the mechanical response of a membrane with pretension. The last term arises from the in-plane stretching of the membrane. The experimentally obtained $F-\delta$ data is fitted to Equation (2) with $E_{\parallel}, F_0, \sigma_0^{2D}$ and δ_0 taken as fitting parameters to extract $E_{\parallel}$ values. Representative data (**Figs. 4D, S2C** and **S2G**) demonstrates excellent agreement between the experimental results and the model, confirming the appropriateness of the model used here.

Figs. 5A-C show the histograms of the measured $E_{\parallel}$ for each MOF tested, which

View Article Online
DOI: 10.1039/D6NR00361C

Open Access Article. Published on 13 April 2026. Downloaded on 4/14/2026 3:06:08 PM.
This article is licensed under a Creative Commons Attribution-NonCommercial 3.0 Unported Licence.

generally follows a Gaussian distribution. **Fig. 5D** summarizes the mean values and standard deviation of the data. $E_{\parallel}$ of 3D-Zn-MOF is 25.9 ± 6.3 GPa, which falls in the range of reported E values of 3D MOFs.[10, 12] In comparison, 2D-Zn-MOF exhibits a much lower $E_{\parallel}$ (11.2 ± 2.5 GPa). Although 3D-Zn-MOF has slightly lower amount of H_2O in the structure, more small molecules filling the porous structure in MOF typically gives higher stiffness.[50] The observed significant reduction in $E_{\parallel}$ is thus unlikely due to the variation in H_2O, but rather arises from the loss of continuous load-bearing connectivity because of the elimination of covalent bonding between the layers (**Figs. 1C, F**), as found in HOIPs,[15] a similar family of materials. In 3D-Zn-MOF, terephthalate linkers integrate adjacent MOF layers into an extended, crosslinked network that efficiently suppresses interlayer slip and distortion of the porous structure. This topological continuity enhances long-range stress transfer, leading to a high effective in-plane stiffness. Upon dimensional reduction to a 2D layered configuration, the absence of vertical bridging linkers can have two softening effects. First, it relaxes some deformation restrictions of the in-plane MOF structure. This relaxation can introduce additional rotational degrees of freedom at the coordination nodes, activating architectural "soft modes" that allow the porous framework to be further deformed, similar to the softening effects arising from distorting the octahedra and the puckered structure in 2D HOIPs[46] and black phosphorous,[51] respectively. Second, eliminating the interlayer linkers permits sliding between adjacent layers upon mechanical loading, which can also reduce the in-plane stiffness, as suggested by prior studies on 2D materials.[32, 33, 35] This further implies

Nanoscale Accepted Manuscript

View Article Online
DOI: 10.1039/D6NR00361C

Open Access Article. Published on 13 April 2026. Downloaded on 4/14/2026 3:06:08 PM.
This article is licensed under a Creative Commons Attribution-NonCommercial 3.0 Unported Licence.

that tuning the interlayer interactions, *e.g.*, by engineering the molecular chemistry and structure of the organic ligands,[46] *via* intercalation chemistry,[52] or through environmental factors like temperature[39, 53] that affect the interacting forces, can effectively tune $E_{\parallel}$ of 2D MOFs, as suggested by our recent studies of 2D HOIPs.[39, 46, 49]

The metal ions are essential components of the coordination nodes in MOF structures and have been widely used to tailor the functional properties of MOF while maintaining a similar porous structure.[6] Surprisingly, although the unconnected 2D layered structure is retained (**Fig. S1**), replacing Zn by Mn greatly increases $E_{\parallel}$ to 25.5 ± 4.9 GPa, which is almost as stiff as 3D-Zn-MOF. This is unlikely due to the absence of H_2O in the 2D-Mn-MOF because inclusion of small molecules into the porous structure should increase $E_{\parallel}$,[50] which contradicts our observation. Similarly, the observed trend is probably not because of the interfaces since the interlayer interaction strength should be comparable owing to the same interfacial chemistry consisting of BDC ligands.

We attributed the change in $E_{\parallel}$ to the deformability of the framework architecture arising from the node coordination difference. Distortion of architectural features plays crucial role in dictating the elastic modulus of 2D materials as shown in black phosphorous and 2D HOIPs. The distortion of the porous MOF structure should be significantly affected by the nodes. In the tested MOF here, the nodes are formed by metal atoms coordinated to the oxygen atoms in the BDC ligands. In 2D-Mn-MOF, the node is formed by three joint Mn-O octahedra (**Figs. 3C** and **S1A**),

Nanoscale Accepted Manuscript

View Article Online
DOI: 10.1039/D6NR00361C

Open Access Article. Published on 13 April 2026. Downloaded on 4/14/2026 3:06:08 PM.
This article is licensed under a Creative Commons Attribution-NonCommercial 3.0 Unported Licence.

while in 2D-Zn-MOF, it constitutes with one Zn-O octahedron connected with two Zn-O tetrahedra (**Figs. 1A** and **3A**). This reduced coordination with BDC links makes the framework weaker and more deformable, and hence results in the structural softness. Tuning the fine features of the connection topology near the coordination nodes can be another effective route to engineer $E_{\parallel}$ of 2D MOFs.

We put the tested materials in this study into a density *vs.* $E_{\parallel}$ Ashby plot, together with other relevant 2D materials and material categories commonly used in engineering applications (**Fig. 6**). Density and Young's modulus are two widely considered properties when one selects materials for applications. Owing to the molecular pores in their structure, MOFs are famous for their relative low density compared to other condensed solids. The results from our study and earlier 2D MOFs measured by proper methods allow us to estimate the boundaries for 2D MOFs on this plot. As shown in **Fig. 6**, 2D MOFs reside closer to polymers, natural materials (*e.g.*, wood) and other hybrid materials (*e.g.*, HOIPs), featuring much lower density and E than metal and ceramics, as a result of the inclusion of organic components and porous structures. The hybrid bonding nature and the structural softness mentioned earlier separate 2D MOFs from conventional 2D materials which have strong, pure inorganic strong bonds in-plane and no/little architectural flexibility under mechanical loading. Because of the similar hybrid bonding nature and structural softness (enabled by distortion of the metal-halide octahedra in HOIPs[46]), $E_{\parallel}$ of 2D HOIPs and 2D MOFs are roughly in the same range, similar to their out-of-plane moduli[15, 54]. However, the absence of porous structure in 2D HOIPs give them slightly higher

Nanoscale Accepted Manuscript

View Article Online
DOI: 10.1039/D6NR00361C

density than 2D MOFs. In comparison, the other 2D family of coordinated polymers, *i.e.,* the covalent-organic frameworks (COFs),[37, 55, 56] are much stiffer, due to the strong covalent bonds that constitute the framework and lack of structural distortion at the nodes owing to the lack of more deformable metal-coordination structures. The absence of heavy metal elements in COFs further reduces their density compared to 2D MOFs. However, the metal elements bestow many functional properties upon 2D MOFs,[6] which will be challenging to engineer into COFs. Generally speaking, 2D MOFs provide material options covering the blank area in the material design space (**Fig. 6**) that balances softness (flexibility), functionality, and light weight to meet application needs.

Conclusions

In conclusion, we employed AFM stretching suspended thin MOF membranes and measured $E_{\parallel}$ of three structurally related, BDC-coordinated MOFs. 3D-Zn-MOF exhibits an $E_{\parallel}$ of 25.9 ± 6.3 GPa, which drops to 11.2 ± 2.5GPa in 2D-Zn-MOF. We attributed the in-plane stiffness reduction to the absence of interlayer covalent bonding, which not only relaxes the in-plane deformation constraints of the MOF but also allows sliding at the interlayer interfaces. In contrast, 2D-Mn-MOF, coordinated by the same BDC linker into a similar topology to 2D-Zn-MOF, shows higher $E_{\parallel}$ (25.5 ± 4.9 GPa). A careful examination of the crystal structure suggests that the enhanced stiffness in 2D-Mn-MOF than 2D-Zn-MOF is likely due to the coordination differences at the node that affect the deformability of the framework architecture. We

Open Access Article. Published on 13 April 2026. Downloaded on 4/14/2026 3:06:08 PM.
This article is licensed under a Creative Commons Attribution-NonCommercial 3.0 Unported Licence.

Nanoscale Accepted Manuscript

View Article Online
DOI: 10.1039/D6NR00361C

Open Access Article. Published on 13 April 2026. Downloaded on 4/14/2026 3:06:08 PM.
This article is licensed under a Creative Commons Attribution-NonCommercial 3.0 Unported Licence.

Nanoscale Accepted Manuscript

further constructed an Ashby plot of density *vs.* E summarizing the major categories of 2D materials and other widely used engineering material systems to guide a general material selection. 2D MOFs offer material options that fill the blank area in the material design space, balancing softness, functionality, and light weight. Our results unveil the critical roles of interlayer interactions and structural deformability in dictating the in-plane stiffness of 2D MOFs, through which the mechanical behavior of 2D MOFs can be tailored leveraging the abundant chemical options available to these materials.

Supporting Information

The Supporting Information is available on the RSC Publications website (https://www.rsc.org/publishing/journals/nanoscale):

- *Details about materials synthesis and x-ray diffraction of the materials investigated, additional AFM images and representative F vs. δ curves, and a summary table of density vs. elastic moduli data used to construct the Ashby plot.*

Author Information

# These authors contributed equally

* Corresponding author:

Dr. Ioannis Spanopoulos: spanopoulos@usf.edu

Dr. Qing Tu: qing.tu@tamu.edu

View Article Online
DOI: 10.1039/D6NR00361C

Accession Codes

Deposition Numbers 2522895-2522896 contain the supplementary crystallographic data for this paper. These data can be obtained free of charge via the joint Cambridge Crystallographic Data Centre (CCDC) and Fachinformationszentrum Karlsruhe Access Structures service.

Acknowledgement

The research was primarily supported by the National Science Foundation under the Award No. CMMI-2311573 (S.Z. and Q. T.). I.S acknowledges support by USF start-up funds.

Open Access Article. Published on 13 April 2026. Downloaded on 4/14/2026 3:06:08 PM.
This article is licensed under a Creative Commons Attribution-NonCommercial 3.0 Unported Licence.

Nanoscale Accepted Manuscript

View Article Online
DOI: 10.1039/D6NR00361C

Open Access Article. Published on 13 April 2026. Downloaded on 4/14/2026 3:06:08 PM.
This article is licensed under a Creative Commons Attribution-NonCommercial 3.0 Unported Licence.

Figures

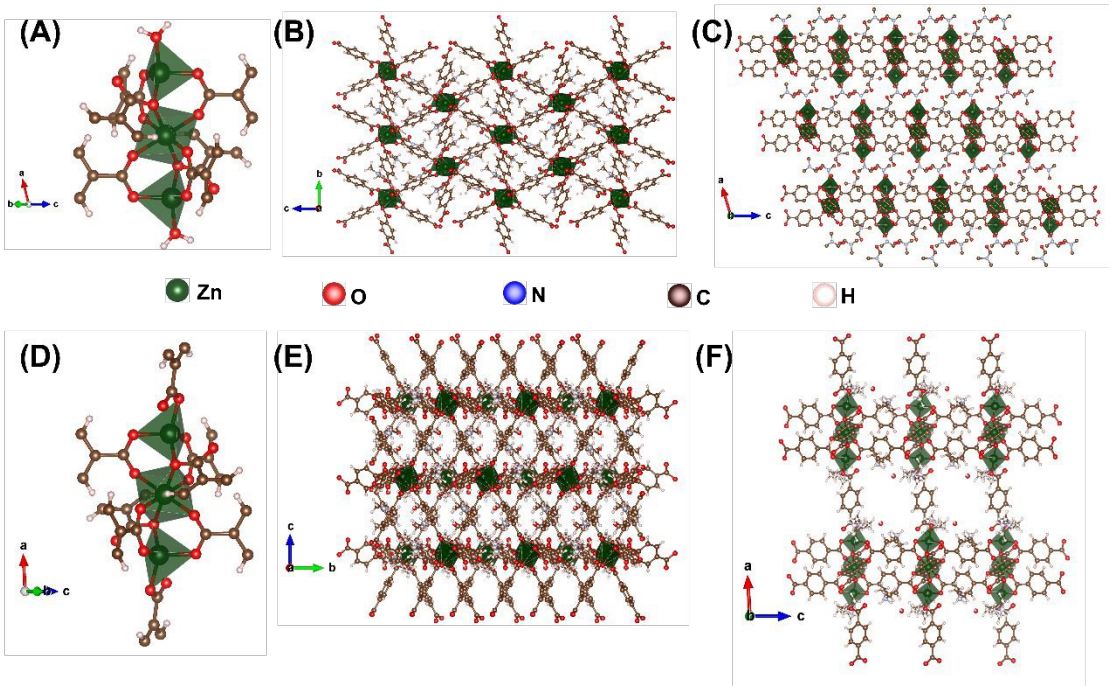

Figure 1. Crystal Structure of the Zn MOFs tested in this study: Top: 2D $Zn_3(BDC)_3(H_2O)_2 \cdot 4(DMF)$; **(A)** The inorganic part of the material and projection of the crystal structure along **(B)** *a*-axis and **(C)** *b*-axis. **Bottom:** 3D $(DMA)_2[Zn_3(BDC)_4 \cdot 1.5H_2O]$; **(D)** The inorganic part of the material and projection of the crystal structure along **(E)** *a*-axis and **(F)** *b*-axis.

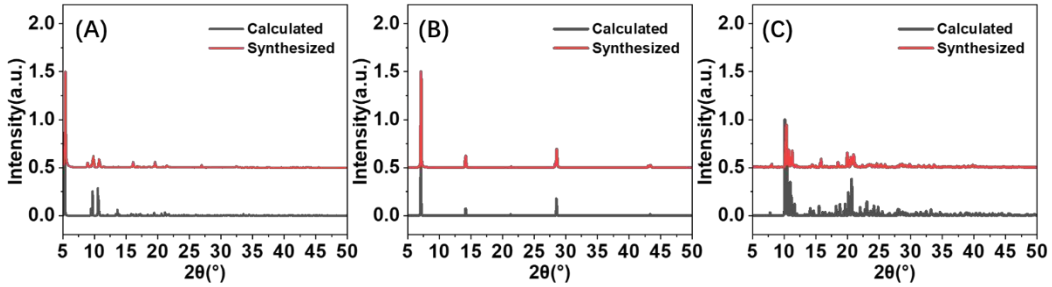

Figure 2. PXRD spectra of tested MOFs: (A) 3D-Zn-MOF, **(B)** 2D-Zn-MOF, and **(C)** 2D-Mn-MOF. The red spectra are calculated from the solved single-crystal structures of the MOFs.

Nanoscale Accepted Manuscript

View Article Online
DOI: 10.1039/D6NR00361C

Open Access Article. Published on 13 April 2026. Downloaded on 4/14/2026 3:06:08 PM.
This article is licensed under a Creative Commons Attribution-NonCommercial 3.0 Unported Licence.

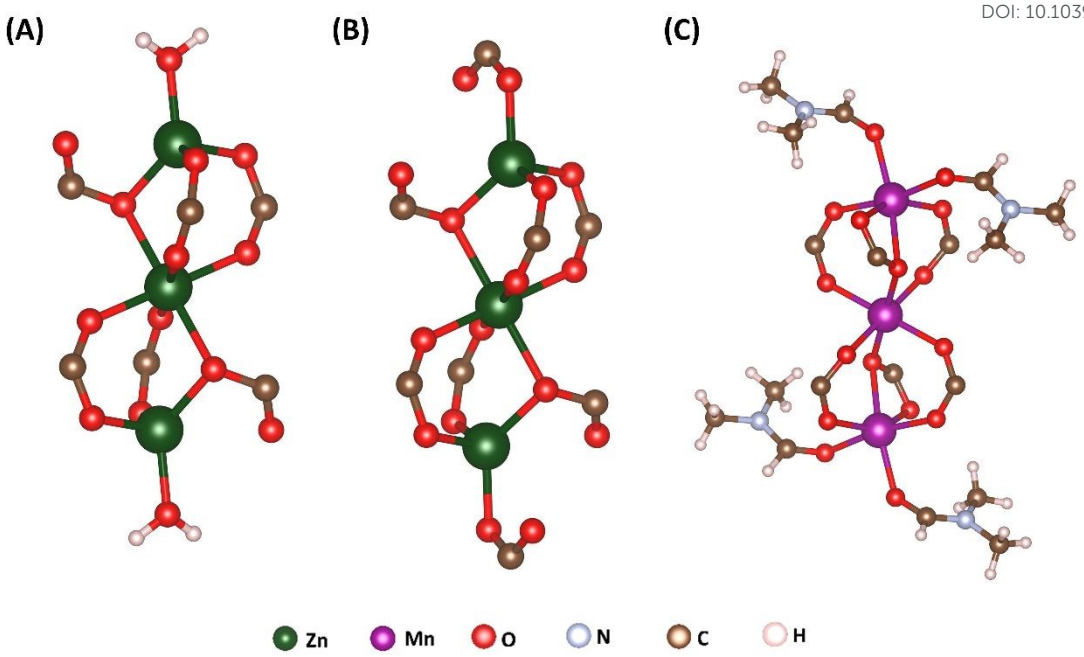

Figure 3. Metal node coordination environment for: (A) 2D-Zn-MOF, **(B)** 3D-Zn-MOF, and **(C)** 2D-Mn-MOF.

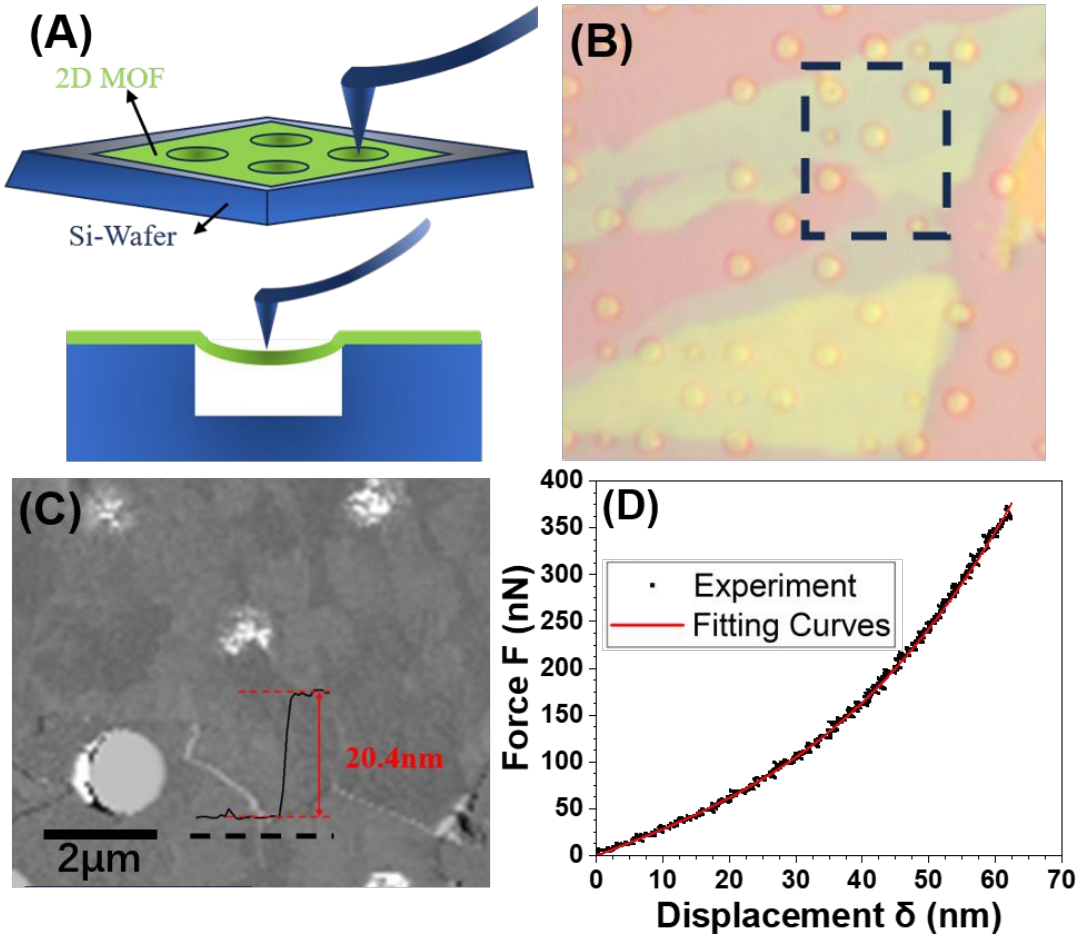

Figure 4. Measuring $E_{\parallel}$ of suspended MOF membranes by AFM: (A) Schematics illustrating AFM stretching suspended thin MOF membranes to extract

Nanoscale Accepted Manuscript

View Article Online
DOI: 10.1039/D6NR00361C

$E_{\parallel}$. **(B)** representative optical image showing thin MOF membranes (2D-Mn-MOF here) transferred on the hole-patterned silicon wafer. **(C)** the tapping mode AFM amplitude image of the region marked by the dashed box in **(B)**. The amplitude image gives a better visualization of the suspended region. The inset is the height profile along the dashed line in **(C)**, showing the thickness of the flake. **(D)** The experimentally obtained $F-\delta$ curve fitted by Equation (2).

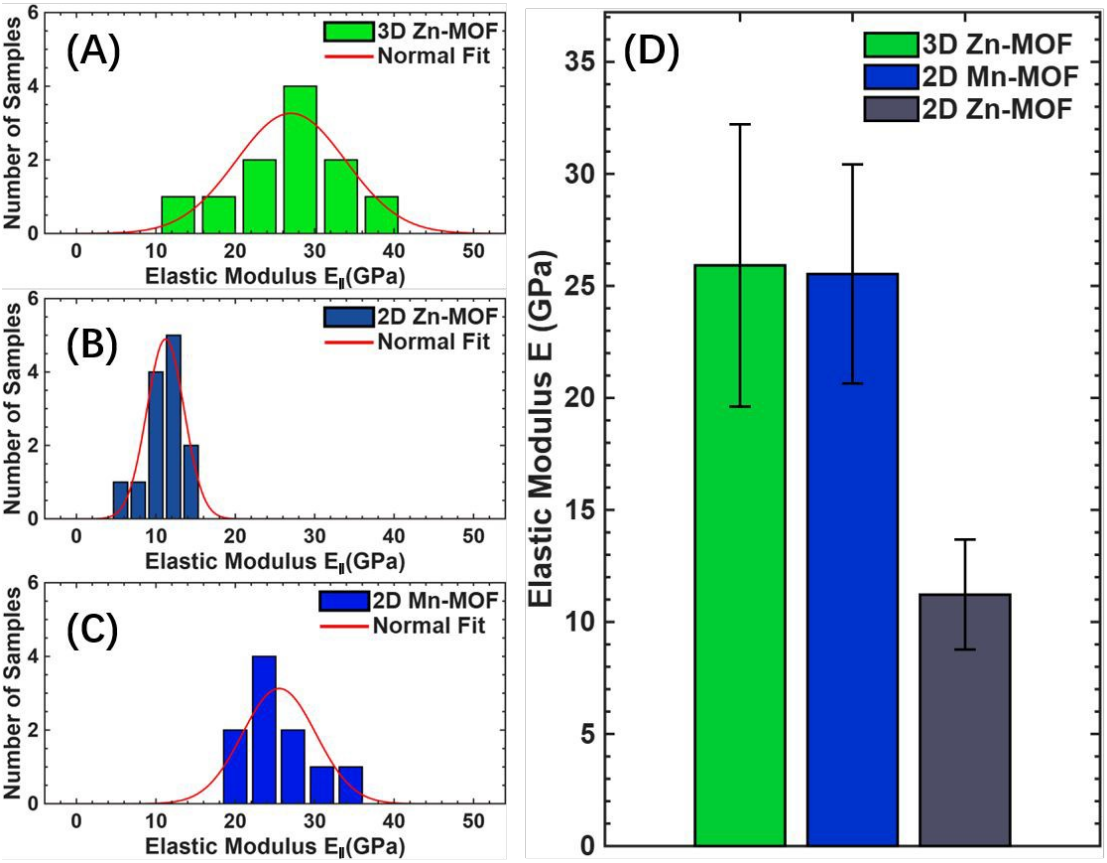

Figure 5. Measured in-plane elastic moduli of MOFs tested here: (A), **(B)** and **(C)** are histograms of the measured elastic moduli data points for 3D-Zn-MOF, 2D-Zn-MOF, and 2D-Mn-MOF, respectively. The histograms are fitted by normal distributions. ***(*D)** mean values and standard deviation of the elastic moduli data measured for each MOF tested here.

Open Access Article. Published on 13 April 2026. Downloaded on 4/14/2026 3:06:08 PM.
This article is licensed under a Creative Commons Attribution-NonCommercial 3.0 Unported Licence.

Nanoscale Accepted Manuscript

View Article Online
DOI: 10.1039/D6NR00361C

Open Access Article. Published on 13 April 2026. Downloaded on 4/14/2026 3:06:08 PM.
This article is licensed under a Creative Commons Attribution-NonCommercial 3.0 Unported Licence.

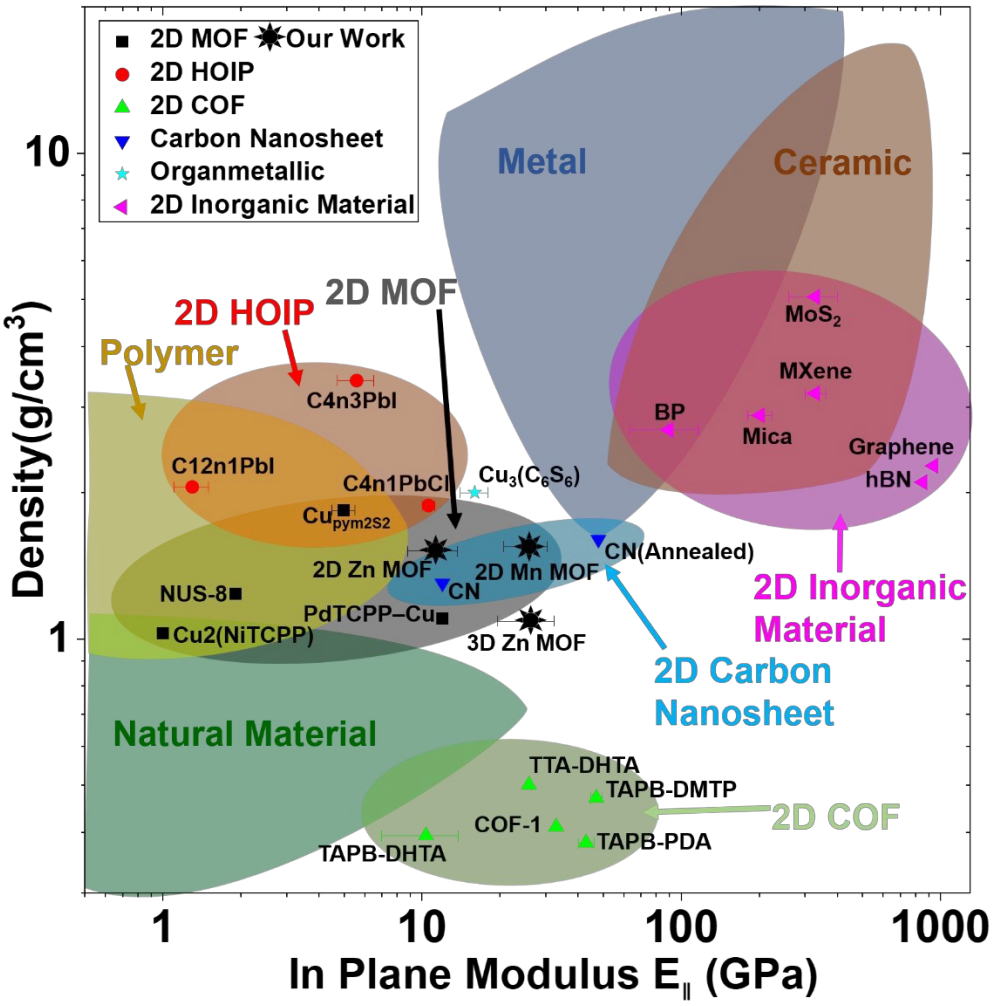

Figure 6. Ashby plot of density vs. $E_{\parallel}$ with tested MOFs, other related 2D materials and main materials used in engineering applications. The ranges for natural materials, polymers, metals and ceramics are adapted from Ref. [57]. The ranges for 2D HOIPs are estimated based on Refs.[35, 39, 46] The material data points marked here and the corresponding references are summarized in **Table S10**.

Nanoscale Accepted Manuscript

View Article Online
DOI: 10.1039/D6NR00361C

Open Access Article. Published on 13 April 2026. Downloaded on 4/14/2026 3:06:08 PM.
This article is licensed under a Creative Commons Attribution-NonCommercial 3.0 Unported Licence.

Nanoscale Accepted Manuscript

References

1. Lee, J.; Farha, O. K.; Roberts, J.; Scheidt, K. A.; Nguyen, S. T.; Hupp, J. T., Metal–organic framework materials as catalysts. *Chemical Society Reviews* **2009,** *38* (5), 1450-1459.

2. Li, B.; Wen, H.-M.; Zhou, W.; Chen, B., Porous Metal–Organic Frameworks for Gas Storage and Separation: What, How, and Why? *The Journal of Physical Chemistry Letters* **2014,** *5* (20), 3468-3479.

3. Qiu, S.; Xue, M.; Zhu, G., Metal–organic framework membranes: from synthesis to separation application. *Chemical Society Reviews* **2014,** *43* (16), 6116-6140.

4. Alekseevskiy, P. V.; Efimova, A.; Povarov, S.; Zhestkij, N. A.; Demakov, P. A.; Burzak, N.; Dyachuk, V. A.; Fedin, V. P.; Potapov, A. S.; Yu, X.; Milichko, V. A., Fiber-Integrated Metal–Organic Framework Nanosheets for Light Emission and Microendoscopy. *ACS Applied Nano Materials* **2026,** *9* (4), 1860-1868.

5. Furukawa, H.; Cordova, K. E.; O'Keeffe, M.; Yaghi, O. M., The Chemistry and Applications of Metal-Organic Frameworks. *Science* **2013,** *341* (6149), 1230444.

6. Chakraborty, G.; Park, I.-H.; Medishetty, R.; Vittal, J. J., Two-Dimensional Metal-Organic Framework Materials: Synthesis, Structures, Properties and Applications. *Chemical Reviews* **2021,** *121* (7), 3751-3891.

7. Alekseevskiy, P. V.; Yu, X.; Efimova, A. S.; Zhestkij, N. A.; Mezenov, Y. A.; Kenzhebayeva, Y. A.; Povarov, S. A.; Lubimova, A.; Bachinin, S. V.; Stepanidenko, E. A.; Dyachuk, V.; Li, N.; Fedin, V. P.; Potapov, A. S.; Milichko, V. A., Ultrathin Lanthanide-Based Metal-Organic Nanosheets with Thickness- and Temperature-Driven Light

View Article Online
DOI: 10.1039/D6NR00361C

Emission. *Laser & Photonics Reviews* **2025,** *19* (12), 2401912.

8. Mezenov, Y. A.; Bachinin, S. V.; Kenzhebayeva, Y. A.; Efimova, A. S.; Alekseevskiy, P. V.; Poloneeva, D.; Lubimova, A.; Povarov, S. A.; Shirobokov, V.; Dunaevskiy, M. S.; Falchevskaya, A. S.; Potapov, A. S.; Novikov, A.; Selyutin, A. A.; Boulet, P.; Kulakova, A. N.; Milichko, V. A., Transformation of 3D Metal–Organic Frameworks into Nanosheets with Enhanced Memristive Behavior for Electronic Data Processing. *Advanced Science* **2025,** *12* (16), 2405989.

9. Swain, G.; Sultana, S.; Parida, K., A review on vertical and lateral heterostructures of semiconducting 2D-MoS2 with other 2D materials: a feasible perspective for energy conversion. *Nanoscale* **2021,** *13* (22), 9908-9944.

10. Tan, J. C.; Cheetham, A. K., Mechanical properties of hybrid inorganic–organic framework materials: establishing fundamental structure–property relationships. *Chemical Society Reviews* **2011,** *40* (2), 1059-1080.

11. Burtch, N. C.; Heinen, J.; Bennett, T. D.; Dubbeldam, D.; Allendorf, M. D., Mechanical properties in metal–organic frameworks: emerging opportunities and challenges for device functionality and technological applications. *Advanced materials* **2018,** *30* (37), 1704124.

12. Redfern, L. R.; Farha, O. K., Mechanical properties of metal–organic frameworks. *Chemical Science* **2019,** *10* (46), 10666-10679.

13. Dziobek-Garrett, R.; Kempa, T. J., Excitons at the interface of 2D TMDs and molecular semiconductors. *The Journal of Chemical Physics* **2024,** *160* (20).

14. Rogge, S. M. J.; Borgmans, S.; Van Speybroeck, V., Absorbing stress via molecular

Open Access Article. Published on 13 April 2026. Downloaded on 4/14/2026 3:06:08 PM.
This article is licensed under a Creative Commons Attribution-NonCommercial 3.0 Unported Licence.

Nanoscale Accepted Manuscript

View Article Online
DOI: 10.1039/D6NR00361C

crumple zones: Strain engineering flexibility into the rigid UiO-66 material. *Matter* **2023,** *6* (5), 1435-1462.

15. Tu, Q.; Spanopoulos, I.; Vasileiadou, E. S.; Li, X.; Kanatzidis, M. G.; Shekhawat, G. S.; Dravid, V. P., Exploring the Factors Affecting the Mechanical Properties of 2D Hybrid Organic–Inorganic Perovskites. *ACS Applied Materials & Interfaces* **2020,** *12* (18), 20440-20447.

16. Jouneghaninaseri, A.; Zhang, S.; Tu, Q.; Liu, J., Molecular engineering in layered metal halide hybrid perovskites for tunable thermal conductivity, elastic modulus, and beyond. *MRS Communications* **2025,** *15* (6), 1307-1322.

17. Oliver, W. C.; Pharr, G. M., An improved technique for determining hardness and elastic modulus using load and displacement sensing indentation experiments. *Journal of Materials Research* **1992,** *7* (6), 1564-1583.

18. Tan, J.-C.; Saines, P. J.; Bithell, E. G.; Cheetham, A. K., Hybrid Nanosheets of an Inorganic–Organic Framework Material: Facile Synthesis, Structure, and Elastic Properties. *ACS Nano* **2012,** *6* (1), 615-621.

19. Iwai, Y.; Kusumoto, S.; Suzuki, R.; Tachibana, M.; Komatsu, K.; Kikuchi, T.; Kawaguchi, S. I.; Kadobayashi, H.; Masubuchi, Y.; Yamamoto, Y.; Ozawa, Y.; Abe, M.; Hirai, K.; Le Ouay, B.; Ohba, M.; Ohtani, R., Mechanical Properties of Modulative Undulating Layers in Two-Dimensional Metal–Organic Frameworks. *Chemistry of Materials* **2024,** *36* (11), 5446-5455.

20. Ji, L.-J.; Qin, Y.; Gui, D.; Li, W.; Li, Y.; Li, X.; Lu, P., Quantifying the Exfoliation Ease Level of 2D Materials via Mechanical Anisotropy. *Chemistry of Materials* **2018,** *30* (24),

Open Access Article. Published on 13 April 2026. Downloaded on 4/14/2026 3:06:08 PM.
This article is licensed under a Creative Commons Attribution-NonCommercial 3.0 Unported Licence.

Nanoscale Accepted Manuscript

View Article Online
DOI: 10.1039/D6NR00361C

8732-8738.

21. Yuan, H.; Li, K.; Shi, D.; Yang, H.; Yu, X.; Fan, W.; Buenconsejo, P. J. S.; Zhao, D., Large-Area Fabrication of Ultrathin Metal-Organic Framework Membranes. *Advanced Materials* **2023,** *35* (18), 2211859.

22. Hermosa, C.; Horrocks, B. R.; Martínez, J. I.; Liscio, F.; Gómez-Herrero, J.; Zamora, F., Mechanical and optical properties of ultralarge flakes of a metal–organic framework with molecular thickness. *Chemical Science* **2015,** *6* (4), 2553-2558.

23. Sahabudeen, H.; Zhang, Q.; Liu, Y.; Heuchel, M.; Machatschek, R., Mechanistic insights into the deformation and degradation of a 2D metal organic framework. *npj 2D Materials and Applications* **2023,** *7* (1), 25.

24. Lu, J.; Yoshida, Y.; Kanamori, K.; Kitagawa, H., Robust Proton Conduction against Mechanical Stress in Flexible Free-Standing Membrane Composed of Two-Dimensional Coordination Polymer. *Angewandte Chemie International Edition* **2023,** *62* (34), e202306942.

25. Zheng, Z.; Ruiz-Vargas, C. S.; Bauer, T.; Rossi, A.; Payamyar, P.; Schütz, A.; Stemmer, A.; Sakamoto, J.; Schlüter, A. D., Square-Micrometer-Sized, Free-Standing Organometallic Sheets and Their Square-Centimeter-Sized Multilayers on Solid Substrates. *Macromolecular Rapid Communications* **2013,** *34* (21), 1670-1680.

26. Sahabudeen, H.; Qi, H.; Glatz, B. A.; Tranca, D.; Dong, R.; Hou, Y.; Zhang, T.; Kuttner, C.; Lehnert, T.; Seifert, G.; Kaiser, U.; Fery, A.; Zheng, Z.; Feng, X., Wafer-sized multifunctional polyimine-based two-dimensional conjugated polymers with high mechanical stiffness. *Nature Communications* **2016,** *7* (1), 13461.

27. Yusuf, V. F.; Malek, N. I.; Kailasa, S. K., Review on metal–organic framework

Open Access Article. Published on 13 April 2026. Downloaded on 4/14/2026 3:06:08 PM.
This article is licensed under a Creative Commons Attribution-NonCommercial 3.0 Unported Licence.

Nanoscale Accepted Manuscript

View Article Online
DOI: 10.1039/D6NR00361C

classification, synthetic approaches, and influencing factors: applications in energy, drug delivery, and wastewater treatment. *ACS omega* **2022,** *7* (49), 44507-44531.

28. Ghasempour, H.; Wang, K.-Y.; Powell, J. A.; ZareKarizi, F.; Lv, X.-L.; Morsali, A.; Zhou, H.-C., Metal–organic frameworks based on multicarboxylate linkers. *Coordination Chemistry Reviews* **2021,** *426*, 213542.

29. Li, H.; Eddaoudi, M.; O'Keeffe, M.; Yaghi, O. M., Design and synthesis of an exceptionally stable and highly porous metal-organic framework. *nature* **1999,** *402* (6759), 276-279.

30. Cavka, J. H.; Jakobsen, S.; Olsbye, U.; Guillou, N.; Lamberti, C.; Bordiga, S.; Lillerud, K. P., A new zirconium inorganic building brick forming metal organic frameworks with exceptional stability. *Journal of the American Chemical Society* **2008,** *130* (42), 13850-13851.

31. Lee, C.; Wei, X.; Kysar, J. W.; Hone, J., Measurement of the Elastic Properties and Intrinsic Strength of Monolayer Graphene. *Science* **2008,** *321* (5887), 385-388.

32. Falin, A.; Cai, Q.; Santos, E. J.; Scullion, D.; Qian, D.; Zhang, R.; Yang, Z.; Huang, S.; Watanabe, K.; Taniguchi, T., Mechanical properties of atomically thin boron nitride and the role of interlayer interactions. *Nature communications* **2017,** *8* (1), 15815.

33. Bertolazzi, S.; Brivio, J.; Kis, A., Stretching and Breaking of Ultrathin MoS2. *ACS Nano* **2011,** *5* (12), 9703-9709.

34. Kim, D.; Qian, E. K.; Chica, D. G.; Chiang, Y.-H.; Kanatzidis, M. G.; Tu, Q., Mechanical Properties of 2D LiInP2Se6: Implication for Semiconductor Applications. *ACS Applied Nano Materials* **2023,** *6* (10), 8214-8221.

Open Access Article. Published on 13 April 2026. Downloaded on 4/14/2026 3:06:08 PM.
This article is licensed under a Creative Commons Attribution-NonCommercial 3.0 Unported Licence.

Nanoscale Accepted Manuscript

View Article Online
DOI: 10.1039/D6NR00361C

Open Access Article. Published on 13 April 2026. Downloaded on 4/14/2026 3:06:08 PM.
This article is licensed under a Creative Commons Attribution-NonCommercial 3.0 Unported Licence.

35. Tu, Q.; Spanopoulos, I.; Yasaei, P.; Stoumpos, C. C.; Kanatzidis, M. G.; Shekhawat, G. S.; Dravid, V. P., Stretching and Breaking of Ultrathin 2D Hybrid Organic–Inorganic Perovskites. *ACS Nano* **2018,** *12* (10), 10347-10354.

36. Kim, D.; Vasileiadou, E. S.; Spanopoulos, I.; Wang, X.; Yan, J.; Kanatzidis, M. G.; Tu, Q., Unveiling the Fatigue Behavior of 2D Hybrid Organic–Inorganic Perovskites: Insights for Long-Term Durability. *Advanced Science* **2023,** *10* (26), 2303133.

37. Fang, Q.; Pang, Z.; Ai, Q.; Liu, Y.; Zhai, T.; Steinbach, D.; Gao, G.; Zhu, Y.; Li, T.; Lou, J., Superior mechanical properties of multilayer covalent-organic frameworks enabled by rationally tuning molecular interlayer interactions. *Proceedings of the National Academy of Sciences* **2023,** *120* (15), e2208676120.

38. Bagherzadeh, M.; Ashouri, F.; Đaković, M., Synthesis, structural characterization and application of a 2D coordination polymer of Mn-terephthalate as a heterogeneous catalyst for olefin oxidation. *Polyhedron* **2014,** *69*, 167-173.

39. Kim, D.; Vasileiadou, E. S.; Spanopoulos, I.; Kanatzidis, M. G.; Tu, Q., Abnormal In-Plane Thermomechanical Behavior of Two-Dimensional Hybrid Organic–Inorganic Perovskites. *ACS Applied Materials & Interfaces* **2023,** *15* (6), 7919-7927.

40. Efimova, A. S.; Alekseevskiy, P. V.; Timofeeva, M. V.; Kenzhebayeva, Y. A.; Kuleshova, A. O.; Koryakina, I. G.; Pavlov, D. I.; Sukhikh, T. S.; Potapov, A. S.; Shipilovskikh, S. A.; Li, N.; Milichko, V. A., Exfoliation of 2D Metal-Organic Frameworks: toward Advanced Scalable Materials for Optical Sensing. *Small Methods* **2023,** *7* (11), 2300752.

41. Walters, D. A.; Cleveland, J. P.; Thomson, N. H.; Hansma, P. K.; Wendman, M. A.;

Nanoscale Accepted Manuscript

View Article Online
DOI: 10.1039/D6NR00361C

Gurley, G.; Elings, V., Short cantilevers for atomic force microscopy. *Review of Scientific Instruments* **1996,** *67* (10), 3583-3590.

42. Hutter, J. L.; Bechhoefer, J., Calibration of atomic - force microscope tips. *Review of Scientific Instruments* **1993,** *64* (7), 1868-1873.

43. Edgar, M.; Mitchell, R.; Slawin, A. M. Z.; Lightfoot, P.; Wright, P. A., Solid-State Transformations of Zinc 1,4-Benzenedicarboxylates Mediated by Hydrogen-Bond-Forming Molecules. *Chemistry – A European Journal* **2001,** *7* (23), 5168-5175.

44. Jiang, Z.; An, Y.; Zhu, X.; Tian, C.; Bai, J.; Li, Y., Solvent-Dependent Synthesis from Layer to Microporous Pillared-Layer Framework for Selective Sorption of Gas Light Hydrocarbons. *Zeitschrift für anorganische und allgemeine Chemie* **2015,** *641* (15), 2599-2603.

45. Batten, S. R.; Champness, N. R.; Chen, X.-M.; Garcia-Martinez, J.; Kitagawa, S.; Öhrström, L.; O'Keeffe, M.; Suh, M. P.; Reedijk, J., Terminology of metal–organic frameworks and coordination polymers (IUPAC Recommendations 2013). *Pure and Applied Chemistry* **2013,** *85* (8), 1715-1724.

46. Kim, D.; Vasileiadou, E. S.; Spanopoulos, I.; Kanatzidis, M. G.; Tu, Q., In-plane mechanical properties of two-dimensional hybrid organic–inorganic perovskite nanosheets: structure–property relationships. *ACS Applied Materials & Interfaces* **2021,** *13* (27), 31642-31649.

47. Castellanos-Gomez, A.; Poot, M.; Steele, G. A.; Van Der Zant, H. S.; Agraït, N.; Rubio-Bollinger, G., Elastic properties of freely suspended MoS2 nanosheets. *arXiv preprint arXiv:1202.4439* **2012**.

Open Access Article. Published on 13 April 2026. Downloaded on 4/14/2026 3:06:08 PM.
This article is licensed under a Creative Commons Attribution-NonCommercial 3.0 Unported Licence.

Nanoscale Accepted Manuscript

View Article Online
DOI: 10.1039/D6NR00361C

48. Komaragiri, U.; Begley, M.; Simmonds, J., The mechanical response of freestanding circular elastic films under point and pressure loads. *J. Appl. Mech.* **2005,** *72* (2), 203-212.

49. Tu, Q.; Kim, D.; Shyikh, M.; Kanatzidis, M. G., Mechanics-coupled stability of metal-halide perovskites. *Matter* **2021,** *4* (9), 2765-2809.

50. Canepa, P.; Tan, K.; Du, Y.; Lu, H.; Chabal, Y. J.; Thonhauser, T., Structural, elastic, thermal, and electronic responses of small-molecule-loaded metal–organic framework materials. *Journal of Materials Chemistry A* **2015,** *3* (3), 986-995.

51. Wei, Q.; Peng, X., Superior mechanical flexibility of phosphorene and few-layer black phosphorus. *Applied Physics Letters* **2014,** *104* (25).

52. Yang, R.; Mei, L.; Lin, Z.; Fan, Y.; Lim, J.; Guo, J.; Liu, Y.; Shin, H. S.; Voiry, D.; Lu, Q.; Li, J.; Zeng, Z., Intercalation in 2D materials and in situ studies. *Nature Reviews Chemistry* **2024,** *8* (6), 410-432.

53. Namakian, R.; Garzon, M. A.; Tu, Q.; Erdemir, A.; Gao, W., Temperature-Induced Phase Transition in 2D Alkylammonium Lead Halide Perovskites: A Molecular Dynamics Study. *ACS Nano* **2024,** *18* (34), 22926-22937.

54. Tu, Q.; Spanopoulos, I.; Hao, S.; Wolverton, C.; Kanatzidis, M. G.; Shekhawat, G. S.; Dravid, V. P., Out-of-plane mechanical properties of 2D hybrid organic–inorganic perovskites by nanoindentation. *ACS applied materials & interfaces* **2018,** *10* (26), 22167-22173.

55. Hao, Q.; Zhao, C.; Sun, B.; Lu, C.; Liu, J.; Liu, M.; Wan, L.-J.; Wang, D., Confined synthesis of two-dimensional covalent organic framework thin films within superspreading water layer. *Journal of the American Chemical Society* **2018,** *140* (38),

Open Access Article. Published on 13 April 2026. Downloaded on 4/14/2026 3:06:08 PM.
This article is licensed under a Creative Commons Attribution-NonCommercial 3.0 Unported Licence.

Nanoscale Accepted Manuscript

View Article Online
DOI: 10.1039/D6NR00361C

12152-12158.

56. Fang, Q.; Sui, C.; Wang, C.; Zhai, T.; Zhang, J.; Liang, J.; Guo, H.; Sandoz-Rosado, E.; Lou, J., Strong and flaw-insensitive two-dimensional covalent organic frameworks. *Matter* **2021,** *4* (3), 1017-1028.

57. Ashby, M. F., *Materials Selection in Mechanical Design* 4th ed.; Elsevier: 2011.

Open Access Article. Published on 13 April 2026. Downloaded on 4/14/2026 3:06:08 PM.
This article is licensed under a Creative Commons Attribution-NonCommercial 3.0 Unported Licence.

Nanoscale Accepted Manuscript

View Article Online
DOI: 10.1039/D6NR00361C

The data supporting this article have been included as part of the Supplementary Information, which will be available on the RSC Publications website (https://www.rsc.org/publishing/journals/nanoscale):

- *Details about materials synthesis and x-ray diffraction of the materials investigated, additional AFM images and representative F vs. δ curves, and a summary table of density vs. elastic moduli data used to construct the Ashby plot.*

Deposition Numbers 2522895-2522896 contain the supplementary crystallographic data for this paper. These data can be obtained free of charge via the joint Cambridge Crystallographic Data Centre (CCDC) and Fachinformationszentrum Karlsruhe Access Structures service.

Open Access Article. Published on 13 April 2026. Downloaded on 4/14/2026 3:06:08 PM.
This article is licensed under a Creative Commons Attribution-NonCommercial 3.0 Unported Licence.

Nanoscale Accepted Manuscript